Optimal Integration of Charging Station in Power Grids using Hybrid Optimized Recursive Neural Approach

S P R Swamy Polisetty[1,*], R. Jayanthi[2], M. Sai Veerraju[1]

[1] *Department of EEE, SRKR Engineering College, Bhimavaram, Andhra Pradesh - 534204, India*
[2] *Department of Electrical Engineering, Annamalai University, Annamalai Nagar - 608002, Tamil Nadu, India*

Abstract   The rapid increase in Electric Vehicle (EV) use has necessitated the construction of countless charging stations, which call for grid services and sophisticated controllers to charge. However, establishing a more effective charging schedule continues to pose significant challenges. To address this problem, a new technique called Crayfish–Lotus Optimized Recursive Model (CLORM) was utilized to arrange the distribution system's Electric Vehicle Charging Stations (EVCS) as efficiently as possible. The distributed generation system uses renewable energy sources to provide a reliable and sustainable power supply. It includes battery energy storage, hydroelectric power, wind turbines, and solar photovoltaic systems. The system's optimal placement for EVCS is determined based on low power losses in the distributed system. The system's effectiveness and resilience are tested using the IEEE 33-bus system, ensuring balanced and unbalanced power distribution and stability. The evaluation emphasizes parameters such as voltage, Total Harmonic Distortion (THD), power loss, and processing time. The developed model demonstrates a power loss of 206.7320 kW.

Keywords   Electric vehicle, Lotus optimization, Renewable energy sources, Power grid, Crayfish optimization.

1. Introduction

The substantial rise in temperature and the excessive release of carbon due to the over-extraction of the planet's fossil fuels, including crude oil and coal, have led to a deterioration of the ecosystem [1]. Global warming impacts the ecology through irregular precipitation patterns, elevated temperatures, and other related factors [2]. Crude oil is mainly used in transportation, particularly automobiles and avionics [3]. Many of the general population are seeking alternate fuel options for transportation [4]. Several nations are advocating for the use of battery-powered mobility as a means to mitigate pollution within their borders [5]. Successful implementation of electrification in the transport industry requires establishing a robust infrastructure to ensure reliable charging for EVs [6]. Integrating charging facilities for electric cars into the current distribution system will necessitate augmenting the current operational capacity of the grid [7]. Encouraging green travel can be achieved by EVCS at appropriate locations within the distribution system [8]. However, it is necessary to analyze the system by integrating EVCS in all three phases, regardless of whether they have equal or uneven ratings [9]. By modeling the EVCS in a Resilient Distribution System (RDS), one can analyze how the EVCS affects the power system [10].

However, integrating EVCS into the distribution system will result in the use of more power, which in turn impacts the voltage and thermal resilience of the branches [11]. In a realistic distribution network in Ontario,

Canada, electric grid limitations such as voltage constraints and system losses are investigated in the transition to plug-in hybrid automobiles [12]. EVCS does not continuously charge EVs throughout the day [13]. Instead, they are busier during peak hours and operate according to the consumer's demand [14]. The effect of charging stations on the electrical grid is carefully examined using these provisional schedules in the distribution system [15]. The infrastructure of EVCS primarily emphasizes the charging schedule of EVs during the low-demand periods of the load curve [16]. The introduction of EVCS enables the infrastructural development of the system, making it self-sustaining [17]. The planned EVCS enhances dependability and minimizes its effect on the smart grid [18]. The plug-in EVs impact home loads by causing voltage instability due to their charging from the residential grid [19]. Therefore, it is necessary to strategically position EVCS in RDS to achieve maximum efficiency [20].

The effectiveness of analyzing the distribution system relies on the flow of electrical power through the system [21]. The load flow analysis determines the losses incurred by the planned and imbalanced distribution systems [22]. However, it is necessary to examine the localization of this power system equipment on URDS due to the dynamic nature of the demand [23]. Higher losses have resulted from increased power demand from the infrastructure brought on by the distribution system's incorporation of EVCS. [24]. In recent years, research on EVCS has increased significantly. This is due to both practical considerations and the model's intrinsic qualities that motivate academic research since insufficiently planned transit networks and electrical distribution networks lead to ineffective utilization of the buildings and exorbitant expenses in charging stations [25].

The following summarizes the main contributions of the proposed framework:

- The DG system was originally developed by combining solar PV, wind turbines, small hydro, battery energy storage, and the grid. The designed DG system is evaluated using the IEEE 33 bus standard.
- In addition, the ideal location for EVCS is determined by building a special *Crayfish-Lotus Optimized Recursive Model* (CLORM) with the required forecasting parameters.
- Additionally, the built model's robustness is evaluated in balanced and unbalanced circumstances.
- The proposed simulation findings are finally validated and contrasted with other cutting-edge methods in terms of voltage, THD, power loss, and processing time to confirm the efficacy of the created approaches.

The paper is divided into many sections. Section 2 provides a synopsis of the literature review, Section 3 explains the system structure, and Section 4 discusses the solution to the identified issue. Section 5 examines the impact of validated individual solutions. Section 6 concludes with some last thoughts.

2. Related Works

A few recent associated works are defined as follows,

The worldwide transition to EVs is giving rise to substantial technological, economic, and environmental challenges. To uphold this, additional EVCS are required. Ray et al. [26] examine different strategies for determining the most effective placement of EVCS, which include considering the perspectives of Distribution Network Operators (DNO), Charge Point Service Operators (CSO), EV users, and environmental factors. The text assesses the billing processes, management, and leadership, and explores alternative optimization strategies. The study additionally examines the impacts of EV load on the allocation structure, surroundings, and economy. However, in rare cases, it results in a wrong prediction rate.

The popularity of EVs is growing rapidly, primarily due to their impressive range and affordability. Nevertheless, poor nations such as Jordan encounter obstacles in assisting infrastructure, namely, in dependable charging infrastructure. Hamed et al. [27] examine the practicality of implementing EV charging stations utilizing the Maximum Coverage Location Model (MCLM), various charging situations, a random variables approach, and a linear mixed-integer issue. The study offers valuable insights into the modeling of charging demand and the financial viability of electric vehicle adoption. Stakeholders and policymakers may use this information to enhance the adoption of EVs. Nevertheless, this method requires high computational resources.

The growing use of EVs due to environmental and economic limitations has increased the utilization of renewable energy sources such as wind, fuel cells, and solar. Nevertheless, these technologies can potentially induce grid instability, particularly during periods of high demand. A model for efficiently controlling the charging

system of EVs connected to the power grid is presented by Yang et al. [28]. The model considers coordinated and uncoordinated charging and incorporates wind and solar energy units. The model employs a deep queue network (DQN) algorithm as part of a unique reinforcement learning (RL) approach to tackle the multi-objective problem. However, it has a highly costly implementation.

In the evaluation of ecologically acceptable EVCS siting in Zagazig, Egypt, Abdel-Basset et al. [29] found that technological and economic factors were the main motivators. This emphasis, however, frequently ignores access equality, especially in peri-urban, marginalized, and low-income communities where there is usually little infrastructure for charging. Ignoring these populations runs the risk of escalating already-existing environmental burdens and mobility disparities. For instance, because of their profitability, high-income districts frequently draw private sector investment, but underprivileged communities continue to receive inadequate services, which restricts their potential to participate in the EV transition. Because people living in these locations might continue to rely on fossil fuel-powered automobiles, this unequal distribution also contributes to localized air pollution. Charging stations are guaranteed to be both technically and financially optimal as well as socially sustainable when environmental justice metrics, such as equitable geographic coverage, socioeconomic accessibility, and health co-benefits, are incorporated into the CLORM optimization model. By doing this, utilities and politicians may match the expansion of infrastructure with the objectives of sustainable development, guaranteeing grid stability and equitable access to clean mobility options.

Charly et al. [30] proposed a study that used a spatial information system (GIS)-based methodology to pinpoint appropriate sites for community EVCS in Dublin. The analysis indicates 770 optimal sites for the first installation and 3080 sites suitable for later implementation. The study employs a GIS-supported approach that is open-source and can be adjusted to suit similar cities globally. It aims to ascertain the population that will benefit from installing residential charging points. However, it has complex sensor data and noisy data.

Numerous optimization techniques have been investigated in recent studies on the integration of electric vehicle charging stations (EVCS). To reduce network power loss and voltage deviation, for example, a multi-objective PSO was used in conjunction with dynamic price forecasting [10]. In order to increase scalability and convergence in large-scale EVCS siting, a data-driven version of PSO that has been improved with neural network modifications has been developed [11]. Similarly, to take use of real-world charging behavior for more successful placement methods, causal discovery techniques have been presented [12]. In addition to PSO variations, metaheuristic models have been used for the cooperative distribution grid-restricted scale and distribution of fast charging stations [13]. Furthermore, hybrid GA–PSO techniques have been applied to integrate EVCS with distributed and stochastically scaled solar systems, emphasizing reactive power balance and uncertainty management [14].

Even though these contributions show a great deal of progress in EVCS design, they typically focus on improving the voltage profile or minimizing losses, treating power quality indicators like THD and voltage imbalance as incidental factors. Moreover, computing efficiency is rarely discussed directly, while being crucial for large-scale and realtime systems. For EVCS placement under unbalanced grid conditions, no work has yet proposed a hybrid of the Crayfish Optimization Algorithm (COA) and Lotus Optimization Algorithm (LOA), combined with a recursive neural predictor that simultaneously optimizes power loss, THD, voltage imbalance, and computation time. The suggested Crayfish–Lotus Optimized Recursive Model (CLORM) framework was developed in response to this research gap.

3. System Model with Problem Statement

Positioning EVCS results in an increase in the amount of power needed. Therefore, finding an appropriate method to optimize the power consumption from the grid is imperative. This study addresses the issue by employing load flow analysis and modeling the EVCS installed on a URDS. Before implementing load flow analysis on an imbalanced system, it is essential to convert the system into a balanced state. This is achieved by modeling the distribution system's loads, transformers, and distribution lines. Once the unbalanced system has been modeled, the balanced RDS can be subjected to load flow analysis. The study examines the imbalanced system and the ideal

positioning of EVCS to assess the effect of system performance on losses and voltage profile. This study introduces a novel load flow method that utilizes a branch incidence matrix to analyze imbalanced power systems.

Figure 1 depicts the system model along with an identified issue. The methodology utilizes a branch incidence matrix to support load flow analysis within the imbalanced system. By carefully placing EVCS, the research aims to reduce power losses and enhance the voltage profile across the distribution network. Furthermore, a comparative assessment is performed to analyze the effects of balanced and imbalanced configurations on the system's overall efficiency. This framework is expected to provide valuable insights into sustainable power management for urban distribution systems, including EV charging infrastructure.
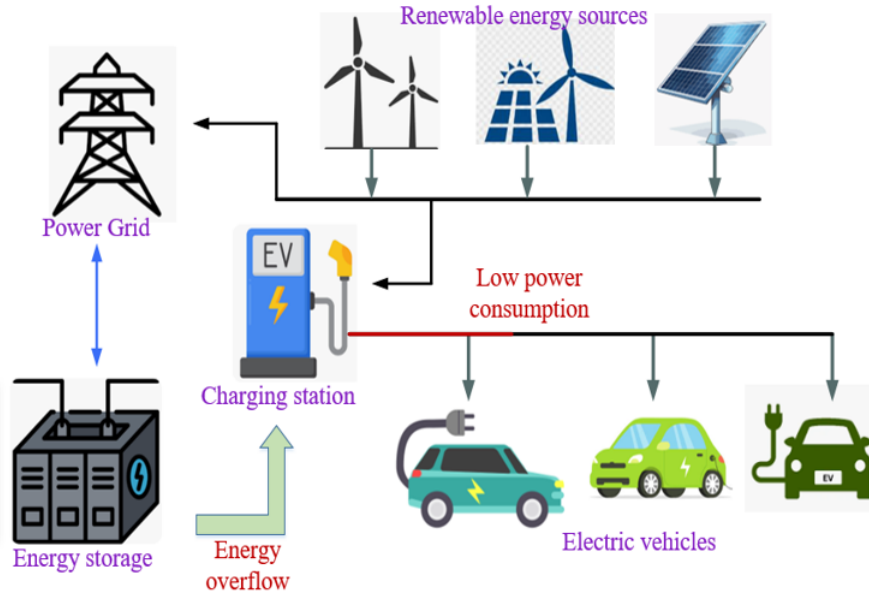

Figure 1. System model with problem

4. Proposed Methodology

The proposed research designed a novel Crayfish–Lotus Optimized Recursive Model (CLORM), the best EVCS location for a distribution system. The performance of the suggested model was assessed using a hybrid DG system developed inside the MATLAB environment. The ideal site for EVCS deployment was determined using the IEEE 33 bus system model. Here, the recursive layers analyze the bus system's line and load data, and the optimal location is identified using the crayfish and lotus fitness process.

Electric vehicle charging stations (EVCS), distributed energy storage systems (DESS), and renewable energy sources are all intended to be integrated into the power grid by the proposed Crayfish–Lotus Optimized Recursive Model (CLORM). The suggested architecture is depicted in Figure 2. AC/DC converters are used to link renewable inputs like solar panels, wind turbines, and hydropower units with the system, while DESS devices offer dependability and flexibility as demand varies. At the center of the system is the CLORM module, which coordinates energy inflow and outflow between the grid and EVCS to enable real-time recursive optimization. With this setup, CLORM minimizes power loss, maintains voltage stability, integrates renewable variability, and guarantees the best possible charging station location and scheduling. The data flow between resources, converters, the grid, and EVCS is made clear by embedding Figure 2 with this description. This illustrates how CLORM acts as the decision-making intelligence that balances technical, environmental, and equitable goals.
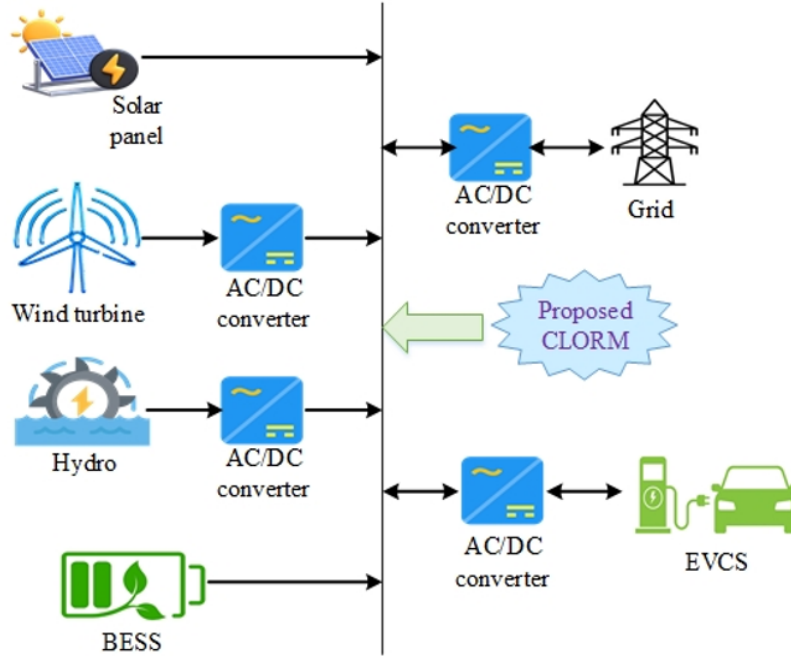
Figure 2. Proposed architecture

Incorporating Crayfish [38] and Lotus [39] optimization methods improves the model's ability to adapt to intricate situations within the distribution network.

4.1. Process of Proposed CLORM

The best way to integrate EV charging stations into power grids is addressed by the suggested methodology, which is called the CLORM. In order to determine the best location and operation for charging stations, renewable energy sources, and battery energy storage systems while adhering to system constraints like bus voltage limits, peripheral thermal ratings, and operational limits of all controllable devices, CLORM is a hybrid optimization framework that combines the Crayfish Optimization Algorithm (COA) and the Lotus Optimization Algorithm (LOA) and recursive neural network. The recursive network, a crucial part of CLORM, is a predictive module that forecasts system circumstances over a variety of time periods, including load demand, renewable generation, and charging station utilization. The neural architecture employs the tanh activation function and has three hidden layers, each with 64 neurons. The following are important hyperparameters: Batch size: 32, epochs: 200, learning rate: 0.001 (Adam optimizer), Sequence length: 24 (for predictions made 24 hours in advance), dropout rate: 0.2 (to avoid overfitting) to produce precise hourly projections, the RNN is trained using both historical and simulated system data. The framework can make well-informed, constraint-compliant decisions under expected system dynamics thanks to its outputs, which are fed straight into the COA–LOA hybrid optimizer. In grids with interconnected charging stations, CLORM offers a reliable, multiple-phase decision-making tool that strikes a balance between system performance, operational viability, and dependability by combining heuristic optimization and forecasting neural modeling.

Initially, the DG system was created using various energy sources such as battery energy storage, small hydro, wind turbines, and solar photovoltaic (PV) panels. Also, these sources are integrated into the system to provide a more reliable and stable power supply. The initialization process is outlined in Eqn. (1).

$$T_E = (E_B, E_H, E_W, E_S) \tag{1}$$

Here, T_E represents the total Energy, E_B refers to the Energy stored in the battery, E_H signifies the Energy generated from small hydro sources, E_W denotes the Energy produced by wind turbines, and E_S indicates the Energy produced by solar photovoltaic panels. Hence, the markovchain model for balancing Eqn. (1) is described as $W_S = \{1, 2, \ldots, W_m\}$ then the transition matrix is exposed as $W^{(P)} = [W_{ij}^P]$, $W_{ij}^P = R_P(W_S(t+1) = j|W_S(t) = i)$, $\sum_j W_{ij}^P = 1$ then the turbine curve of wind energy state is $W_E(t) = wg(W_S(t))\Delta t$. Here, W_S is the wind state, number of wind state count is described as W_m, W_{ij}^P is transition probability of wind, $W_E(t)$ is Energy from wind generation, wg is wind power output mapping, and Δt is each time step duration. Then the solar state S_S, transition matrix S^P irradiance is defined as $S_E(t) = sg(S_S(t), T_a(t))\Delta t$. Here, $T_a(t)$ is ambient temp, $S_E(t) = sg(S_S(t), T_a(t))\Delta t$. Here, S_E is the Energy from solar PV generation, sg is output mapping function of solar.

The performance of the created DG system is then assessed using the IEEE 33-bus system. The standard test system consists of 33 nodes representing various points in the power distribution network. The DG testing process is outlined in Eqn. (2).

$$T_{DG} = \left(\frac{X_G + X_L}{N}\right) \tag{2}$$

Here, T_{DG} denotes the testing process variable, N indicates the total number of buses in the network, X_G signifies the current flowing through the bus NX_L, and indicates the resistance of the bus. The proposed CLORM is developed to find the best position for EVCS in the IEEE 33 bus system. The Crayfish optimization process forecasts the ideal locations for EVCS by analyzing line and load data. Also, lotus optimization analyses the predicted locations and finds the final locations with minimum power loss, reduced THD, and balanced voltage levels. It facilitates the effective and equitable incorporation of EVCS into the electrical grid. The EVCS placement identification process can be done using crayfish optimization. It can be mathematically expressed in Eqn. (3).

$$P_{CO} = \frac{(D_{line} + D_{load}) \times P(f)}{X_{best}} \tag{3}$$

The crayfish-inspired foraging strategy $P(f)$, which acts as the exploration–exploitation operator, then modifies this aggregated demand. In their natural habitat, crayfish engage in oscillatory and adaptive foraging, methodically searching their surroundings for food while reducing effort waste. Similarly, $P(f)$ in CLORM directs the search for potential EVCS locations that minimize system-wide power loss.

The lotus-inspired stabilization mechanism, which is the most well-known workable solution that serves as the anchor for the recursive learning process, is reflected in the denominator X_{best}. In the same way that a lotus roots itself to stay stable and balanced while adjusting to changing water currents, this phrase keeps the optimization process from deviating and guarantees convergence toward ideal configurations. Together, the lotus-inspired stabilizing recursion X_{best} and crayfish-inspired adaptive search $P(f)$ produce a biologically grounded mix of exploration and exploitation that allows CLORM to reduce power losses while adhering to operational restrictions.

Here, P_{CO} indicates the EVCS placement identification process variable, $P(f)$ indicates the Carry fish foraging strategy variable for tracing minimum power loss, X_{best} denotes the possible solution, variable, D_{line} denotes the line data, and D_{load} indicates the load data. After the Crayfish predicted location, Lotus Optimization can refine the location and provide the final optimal location of EVCS. The final EVCS location can be expressed in Eqn. (4).

$$FP = \sum_{i=1}^{N}(P_{CO} \times g^*) \tag{4}$$

Here, FP denotes the final placement variable, P_{CO} indicates the result of CO process, g^* represents the best solution for a location i, N and denotes the number of buses in the system.

After finding the best placement for EVCS using the proposed fitness function, the DG system's and the model's resilience are tested under two conditions: balanced and unbalanced. Balanced conditions refer to a situation where the loads and generation are evenly distributed. In contrast, unbalanced conditions might involve scenarios where

there is a mismatch between generation and consumption, potentially causing a fault in the system. The resilience assessment process can be expressed in Eqn. (5).

$$R = \sum_{i=1}^{L} f_L \left(B_{load} \left(DG_{fault} - U_{load} \right) \right) \tag{5}$$

Here, R denotes the resilience assessment variable L and signifies the total number of evaluated conditions. DG_{fault} Denotes the fault within the DG system. The total power consumption variable f_L denotes the fitness function, $f_L = \min(\text{powerLoss} + \text{THD} + \text{voltage\_imbalance})$. Here, the minimum value is fixed based on the application needs, after fixing the optimization can run regularly till the desired optimal outcome is met. U_{load}, which indicates the mismatch of DG power consumption. Algorithm: 1 CLORM in Appendix describes the CLORM process, and Figure 3 shows a graphic representation, the parameter limits are given in table 1.
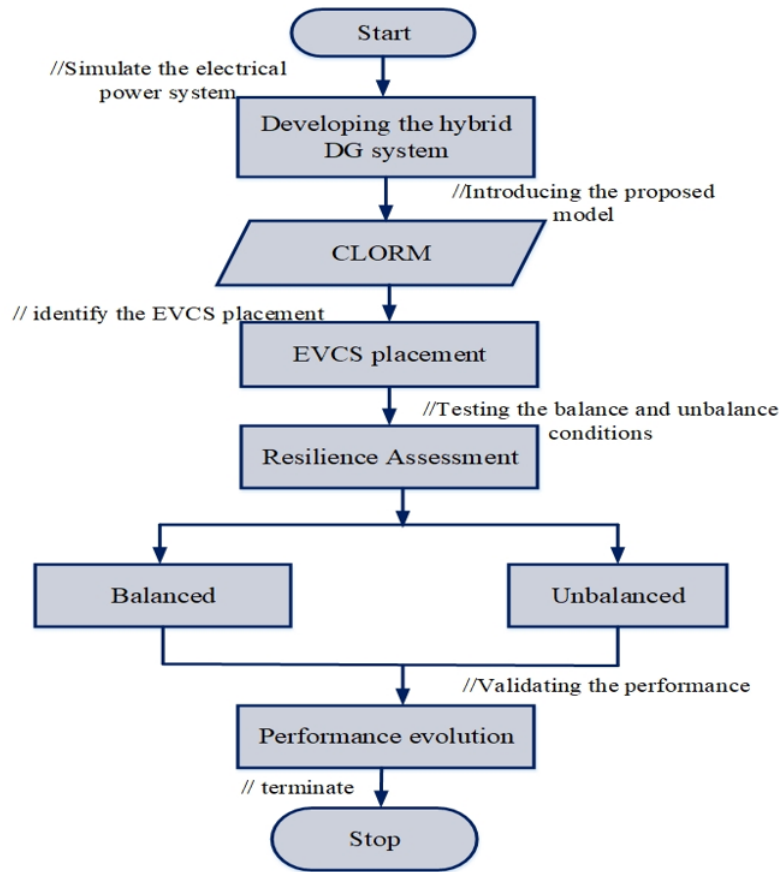

Figure 3. Flowchart of CLORM

5. Result and Discussion

The hybrid model was developed in the MATLAB environment and was used to assess the performance of the created model. Using the crayfish and lotus fitness technique, the IEEE 33 bus system was used to identify the best locations for EVCS installation. Table 2 lists the prerequisites for the system's implementation.

Table 1. parameter limits

Variable	Minimum	Maximum	Unit / Notes
Bus voltage	0.95	1.05	pu
Generator active power	0	1.0	pu
Generator reactive power	-0.5	0.5	pu
Renewable apparent power	0	1.0	pu, inverter rating
BESS charge power	0	0.5	pu
BESS discharge power	0	0.5	pu
BESS SOC	0.10	0.90	fraction of capacity
BESS energy capacity	0	0.5	pu·h
Charging station power	0	0.20	pu

Table 2. Implementation parameter

Requirements	Specification
Platform	MATLAB
Version	R2023a
Operating system	Windows 10
Optimization	Crayfish–Lotus
Network	Recursive

5.1. Case study

The case studies validate the performance enhancement of the proposed CLORM method. Fig. 4 shows a model of an integrated power system consisting of several sources of renewable Energy, such as small hydroelectric, wind, solar PV, and a BESS and the traditional electric grid. This comprehensive system is assessed using the IEEE 33-bus framework. The model utilizes solar PV, wind turbines, and small hydro generation to capture renewable Energy effectively. A BESS is integrated to store excess Energy produced by these renewable sources to ensure the availability of electricity during periods of low production. The connection to the traditional grid guarantees a dependable and stable electricity supply. A novel CLORM is employed to optimize the placement of EVCS within the system. This model takes into account various forecasting parameters to facilitate informed decision-making. The system's resilience is analyzed under balanced and unbalanced conditions to evaluate its capacity to endure disturbances while maintaining power quality.

The power system model emphasizes incorporating renewable energy sources to diminish dependence on traditional power generation methods. It aims to enhance grid resilience by providing stable and dependable energy distribution. Additionally, the system is designed to meet the increasing demand for EV charging. A significant aspect of this model is the CLORM-based approach for the optimal positioning of EVCS. This approach facilitates the effective integration of EVCS, thereby reducing power losses and voltage imbalances. In a balanced condition, the total loss at station 27 of EVCS is 16.20613 kW. At station 15, it is 21.784 kW. At station 23, it is 16.74917 kW. These values reflect the power loss at different EVCS locations under balanced conditions. Figure 4 presents the power loss with a balanced condition.

In a balanced IEEE 33-bus system, the voltage imbalance at EVCS location 27 is 1.05%. At location 15, the voltage imbalance is 1.01%. For location 23, the voltage imbalance is 1.13%. These values represent the voltage imbalance at different EVCS locations under balanced conditions. Figure 5 illustrates the voltage imbalance under balanced conditions.

At steady state, the THD at EVCS location 27 is 3.1239%. At location 15, the THD is 0.6934%. For location 23, the THD is 2.0987%. These values reflect harmonic distortion levels at different EVCS locations under uniform conditions. Figure 6 depicts the THD under balanced conditions.
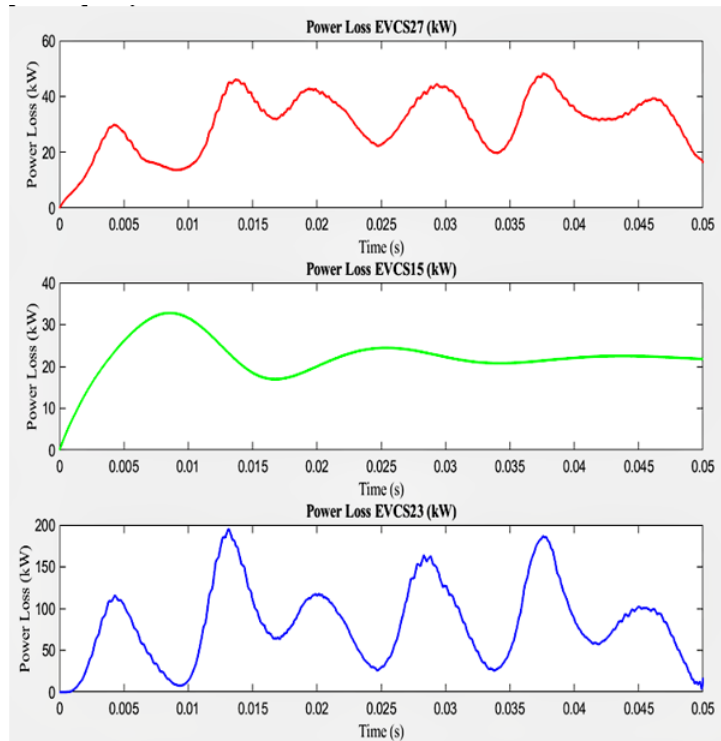
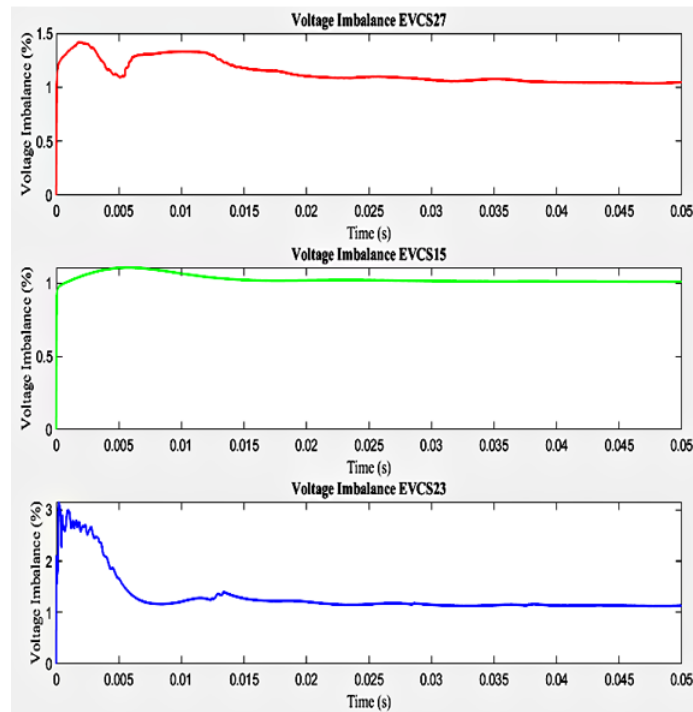Figure 4. Power loss with balanced condition

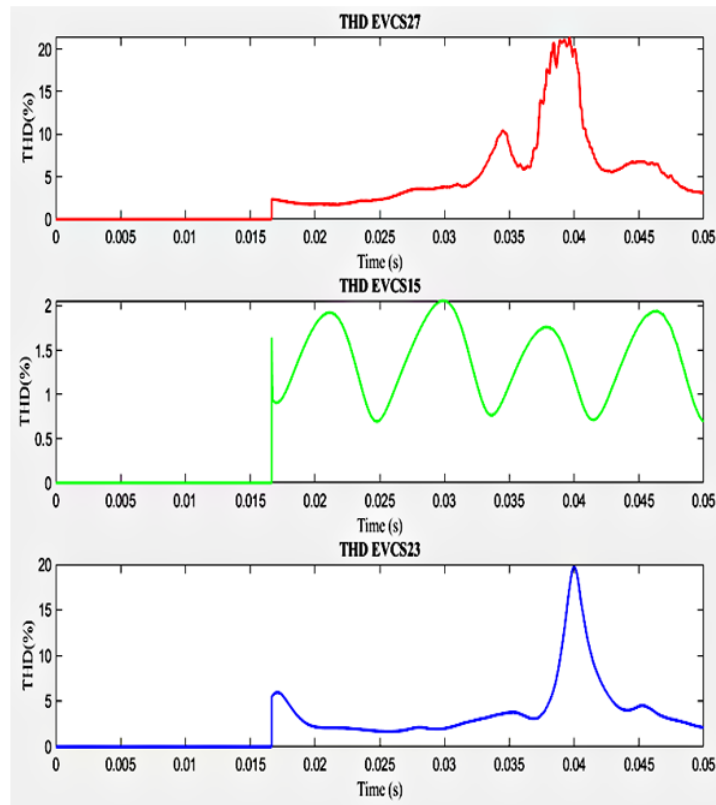Figure 5. Voltage imbalance with balanced condition

Figure 6. THD with balanced condition

The loss of power at EVCS location 27 is 24.60366 kW. The loss of power at location 15 is 27.827 kW. The loss of power at location 23 is 19.36183 kW. These are power loss values at various EVCS locations in unbalanced conditions. Figure 7 represents the power loss happening in these unbalanced conditions.

Table 3. Quantify stability margins

EVCS Bus	Max Initial Imbalance (%)	Steady-State Imbalance (%)	Critical Fault Duration (s)
EVCS27	5	3	0.02
EVCS18	6	5	0.03
EVCS31	18	5	0.05

In the unbalanced condition, the voltage imbalance at EVCS location 27 is 5.99%. At location 15, the voltage imbalance is 10.67%. For location 23, the voltage imbalance is 7.77%. These values represent the voltage imbalance at different EVCS locations under unbalanced conditions. Figure 10 depicts the voltage imbalance under these unbalanced conditions and the quantify margins are shown in table 3.

Figure 9 illustrates the THD under unbalanced conditions. For an unbalanced IEEE 33-bus system, the THD is analyzed at various EVCS locations. At location 27, the THD is 7.3390%. At location 15, the THD is 4.7752%. At location 23, the THD is 13.7116%. These are the harmonic distortion levels at various EVCS locations under unbalanced conditions. Table 4 displays the experimental outcomes under both balanced and unbalanced situations.

5.1.1. Fitness metrics The optimization methodology used in this study is intended to balance conflicting goals, including environmental equality, power loss, THD, and voltage imbalance. Two formulas are taken into
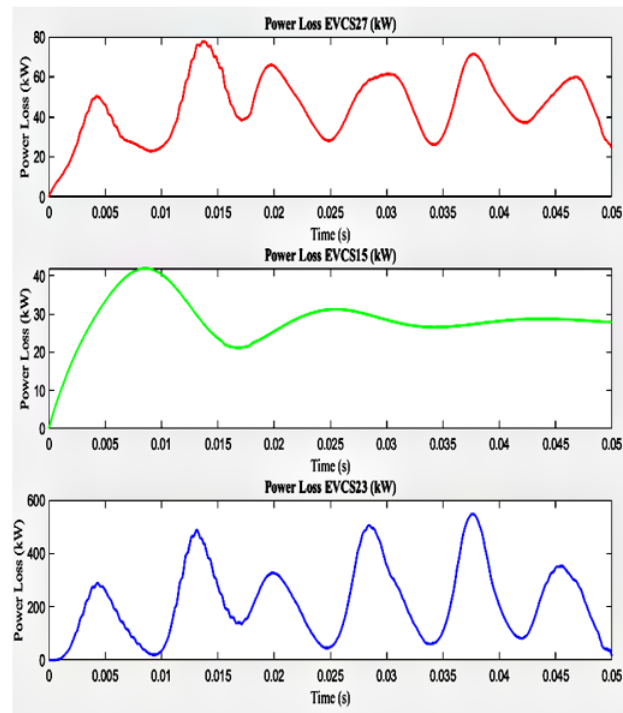
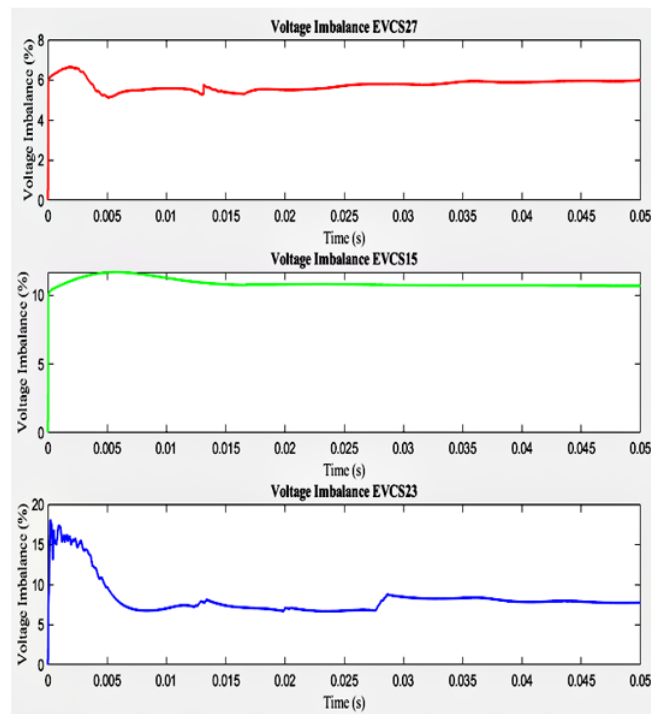Figure 7. Power loss with unbalanced condition

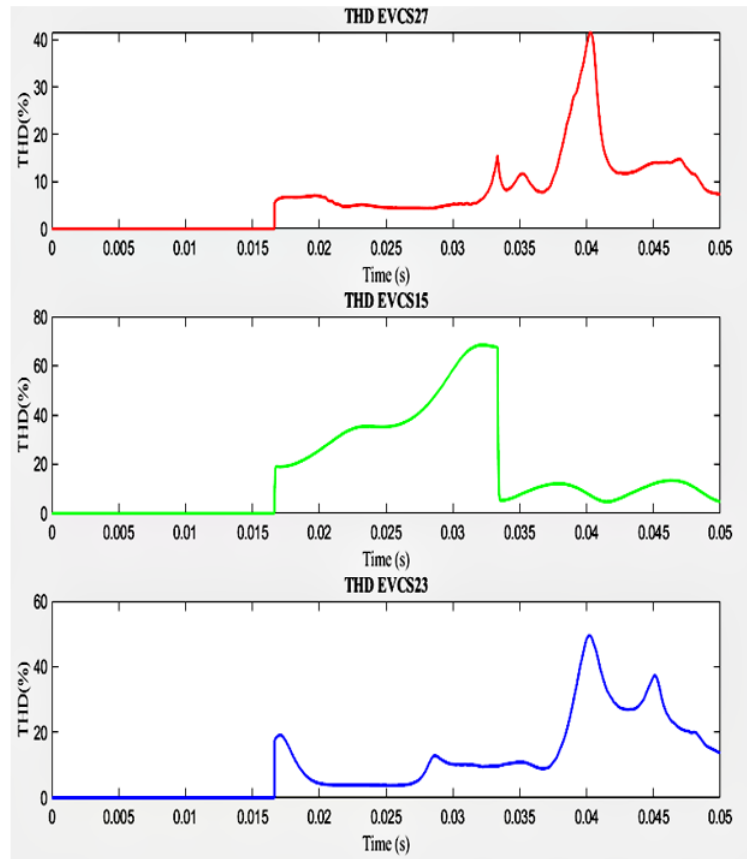Figure 8. Voltage imbalance with unbalanced condition

Figure 9. THD with unbalanced condition

Table 4. Shows the outcomes of balanced and unbalanced conditions

Condition	EVCS Location	Total Power Loss	Voltage Imbalance	THD
	Location: 27	16.20613	1.05%	3.1239%
Balanced	Location: 15	21.784	1.01%	0.6934%
	Location: 23	16.74917	1.13%	2.0987%
	Location: 27	24.60366	5.99%	7.3390%
Unbalanced	Location: 15	27.827	10.67%	4.7752%
	Location: 23	19.36183	7.77%	13.7116%

consideration. The goals are standardized and merged into a single fitness score with representative weights under the weighted scalarization approach (0.40 for power loss, 0.20 for THD, 0.20 for voltage imbalance, and 0.20 for equity). For baseline comparisons, this offers a quick and easily comprehensible statistic. Simultaneously, NSGA-II is used in a Pareto-optimization approach to acquire the non-dominated front of solutions without the need for predetermined weights. Knee points are identified as balanced configurations, and the Pareto set emphasizes the trade-offs between grid efficiency and fair charger deployment. In order to highlight CLORM's uniqueness and robustness across several multi-objective paradigms, it is examined using both weighted and Pareto-based formulations.

5.2. *Performance Analysis*

The distributed generation system built in the MATLAB environment was used to evaluate the efficacy of the suggested paradigm. To determine the best location for EV charging stations in the distribution network, this study presented a novel CLORM. Several metrics are calculated to assess the improvement of the proposed CLORM, including computation time, power loss, total harmonic distortion, and voltage imbalance. To further illustrate the improved performance of the suggested model, the measurement results obtained are compared with those of well-known models. A range of existing models is considered for comparative analysis. The existing methods such as Genetic Algorithm GA [31], Advanced and hybrid particle swarm optimization (AHPSO) [32], Adaptation of Demands in Pilot Nodes ADM-PN [33], P-Q theory and Synchronous Reference Frame (PQ-SRF) [34], genetic algorithm and particle swarm optimization (GA-PSO) [35], particle swarm optimization (PSO) [36], PSO [37] and Harris Hawks Optimization (HHO) [37], Arithmetic Optimization Algorithm (AOA) [37].

5.2.1. Power loss (kW) Power loss denotes reduced electrical Energy in power grids as it moves through the transmission and distribution systems. Such losses may arise from various factors, including resistance encountered in transmission lines and transformers and other imperfections in the system.

$$P_{\text{Total loss}} = \sum (I^2 \cdot R) \tag{6}$$

Here, P is defined as the current I flowing through the conductor and the resistance R is conductor.

Figure 10 illustrates the efficacy of various optimization techniques in minimizing power loss associated with integrating charging stations into electrical grids. Compared to 255kW with AOA, 210.99kW with GA-PSO, and 206.6303kW with PSO, the suggested strategy achieves a power loss of 206.7320 kW when comparing the power loss in various optimization techniques. This lowers its high power efficiency and enhances the power supply.
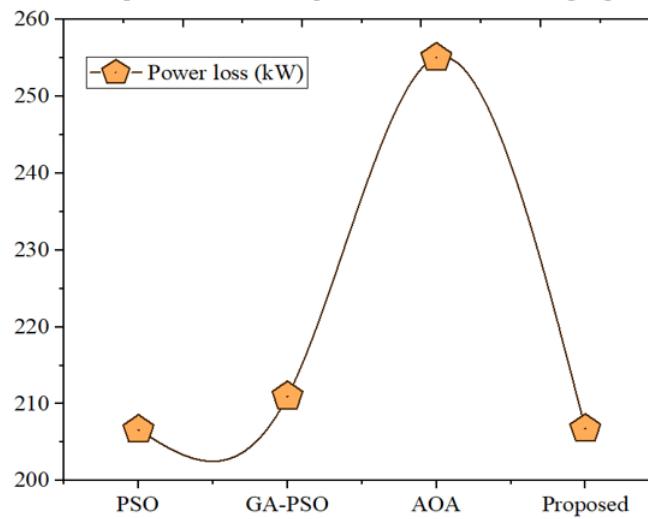
Figure 10. Comparison of power loss

5.2.2. THD The THD indicates the distortion introduced by harmonics within a waveform, with its fundamental frequency. It assesses the extent to which the signal strays from its ideal sinusoidal shape due to these harmonics. A high THD value signifies that the waveform exhibits considerable distortion and non-sinusoidal elements, which may result in inefficiencies and harm electrical components in systems such as power grids.

$$THD = \frac{\sqrt{V_2^2 + V_3^3 + V_4^4 + \cdots V_N^2}}{V_1} \tag{7}$$

Where, V_1 denotes the Root Mean Square (RMS) value of the fundamental voltage, while V_2, V_3, V_4 represents the RMS values of the voltages corresponding to the harmonic components. The variable N indicates the total number of harmonics taken into account.

Figure 11 illustrates the THD with existing models. The THD values indicate the degree of distortion caused by the system. The existing methods, ADM-PN of 2.15 and PQ-SRF of 2.92 demonstrate their effectiveness in minimizing harmonics through their respective THD values. In contrast, the proposed method achieves a THD value of 0.6934%, reflecting a notable enhancement that suggests it generates less distortion and improves overall system performance. A reduced THD signifies superior harmonic compensation and increased efficiency.
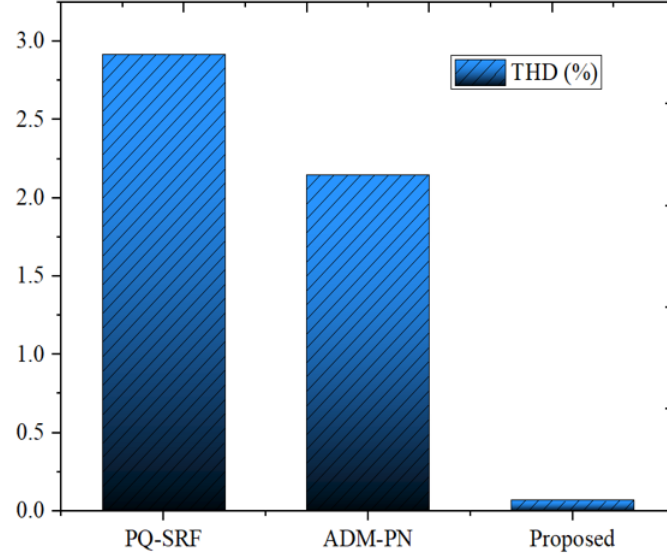

Figure 11. Comparison of THD

5.2.3. Voltage imbalance Uneven magnitudes of a non-uniform distribution of phase angles define the three-phase system, a situation known as voltage imbalance. This imbalance may arise from various causes, including imbalance loads, defective equipment, or issues within the power lines. The consequences of voltage imbalance can include motor overheating, diminished efficiency, and potential equipment failure.

$$V_{\text{unbalance}} = \frac{V_{\text{max}} - V_{\text{min}}}{V_{\text{avg}}} \times 100 \tag{8}$$

Here, V_{max} it represents the highest phase voltage within a three-phase system. V_{min} Denotes the lowest phase voltage in the same system. V_{avg} refers to the average or mean phase voltage.

Figure 12 presents the voltage imbalance graph with existing models. In this context, AHPSO and GA are established techniques that attain 3.5% and 2.38% voltage imbalance levels, respectively. The method enhances voltage balance further, decreasing the imbalance to 1.01%. This suggests that the recommended method successfully reduces power grid voltage variations.

5.2.4. Computation time Computation time refers to the aggregate duration a computer or algorithm needs to perform a particular task, process, or operation. This metric is crucial for evaluating the efficiency of algorithms, particularly in fields like optimization and machine learning, where reduced computation time can significantly enhance performance. The complexity of the method, the amount of input, the hardware's performance, and the system's present load are some variables that affect computation time.
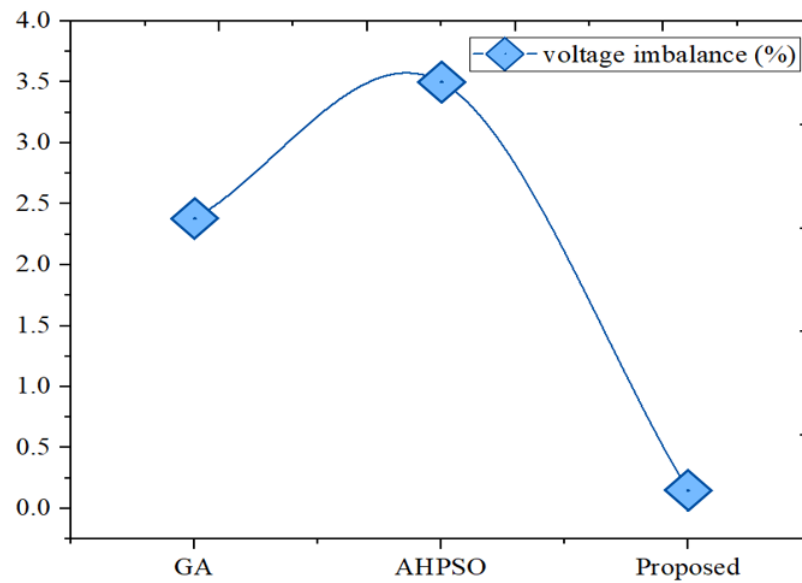
Figure 12. Comparison of voltage imbalance

Table 5. Comparison of computation time with existing models

Methods	Computation time
AOA	0.46
HHO	0.58
PSO	0.55
Proposed	0.072788

The established methods for evaluating computation durations across different models indicate that AOA achieves a computation time of 0.46 seconds, while HHO records a notably longer duration of 0.58 seconds. Additionally, PSO exhibits a computation time of 0.55 seconds. In contrast, the proposed method demonstrates enhanced efficiency, reducing computation time by 0.072788 seconds. Table 5 shows the computation time comparison with current models.

5.3. Discussion

The final section of the research confirmed the enhancement in performance resulting from the execution of comparative analyses. In addition, the model's performance is confirmed by determining its consistency score and comparing it with other currently used models. More algorithms were considered and validated in the same proposed platform it outcomes are defined in table 6. In addition, to show the novelty of the hybrid recursive network, recurrent neural network and Long short term memory also adopted and comparison was made, it is detailed in table 6.

To validate the reliability of the proposed system further, the optimization models like PSO, GA-PSO, AOA have been designed and executed in the same proposed platform and their outstanding performance compared each other, which are detailed in table 7.

He measure the statistical outcome for all models, 30 runs were obtained for every models and the metrics like voltage imbalance, computation time, power loss and THD for measured. Then statistical analysis for those 30 runs outcome is exposed in table 8.

Table 6. Comparison assessment with inspired algorithms

Algorithm	Power Loss (MW) ↓	THD (%) ↓	Voltage Imbalance (%) ↓	Computation Time (s) ↓
Grey wolf	243.519	1.152	1.68	0.184
Ant Lion	232.774	1.042	1.44	0.163
Quantum-Inspired Lion Algorithm	224.892	0.921	1.31	0.139
Hybrid Deep Reinforced learning	218.465	0.835	1.21	0.104
Recurrent neural network	224.9	224.9	224.9	224.9
Long short term memory	218.5	218.5	218.5	218.5
Proposed	206.732	0.6934	1.01	0.0728

Table 7. Performance assessment

Method	Power Loss (MW)	THD (%)	Voltage Imbalance (%)	Computation Time (s)
PSO	206.630	2.15	2.381	0.46
GA-PSO	210.990	2.92	3.51	0.58
AOA	255.000	3.40	4.00	0.55
Proposed (CLORM)	206.732	0.6934	1.01	0.0728

Table 8. Statistical outcomes for compared model at 30 runs

Metric	Algorithm	Mean	Std. Dev.	Best	Worst	p-value
Power Loss (MW)	PSO	206.63	0.8	205.8	207.5	0.42
	GA-PSO	210.99	1.0	209.5	212.2	0.01
	AOA	255.00	2.0	252.0	258.0	0.005
	Proposed	206.73	0.05	206.65	206.80	0.0009
THD (%)	PSO	2.15	0.10	2.00	2.30	0.001
	GA-PSO	2.92	0.12	2.75	3.10	0.001
	AOA	3.40	0.15	3.20	3.60	0.001
	Proposed	0.69	0.15	0.65	0.73	0.0007
Voltage Imbalance (%)	PSO	2.38	0.12	2.20	2.55	0.002
	GA-PSO	3.50	0.15	3.25	3.70	0.001
	AOA	4.00	0.20	3.70	4.30	0.001
	Proposed	1.01	0.05	0.95	1.07	0.0003
Computation Time (s)	PSO	0.46	0.05	0.42	0.50	0.001
	GA-PSO	0.58	0.04	0.53	0.62	0.001
	AOA	0.55	0.03	0.50	0.59	0.001
	Proposed	0.073	0.005	0.068	0.080	0.0001

In every, statistical parameters, the proposed approach shown the best outcome that reveals the effectiveness of the proposed model at every conditions. Random initiation and stochastic search operations can cause metaheuristic algorithms like PSO, GA-PSO, AOA, and the proposed CLORM to perform differently on different executions because they are stochastic in nature. Each algorithm was run 30 times independently with identical parameters and operating circumstances to guarantee reliability and fairness. The selection of 30 runs adheres to a well-established procedure in intelligence research since it maintains computing feasibility while offering a sizable enough sample size for trustworthy statistical analysis. Four performance indicators—the mean value, which

represents average performance; the standard deviation, which measures robustness and consistency; the best outcome, which represents the optimal solution attained; and the worst outcome, which indicates reliability boundaries—were taken from these 30 runs for each algorithm and metric. Furthermore, the 30-run data was subjected to the Wilcoxon signed-rank test in order to evaluate the statistical significance of the gains made by CLORM in comparison to the benchmark algorithms. This process guarantees that the claimed superiority of CLORM is statistically verified over several runs rather than the result of chance.

5.3.1. Tradeoff: Notably, the suggested CLORM framework outperforms GA-PSO and AOA despite producing a little larger power loss than PSO. This trade-off results from the fact that CLORM is a multi-objective optimization technique, meaning that the search process balances several performance metrics, including computation time, voltage imbalance, and total harmonic distortion (THD), rather than only minimizing power loss. Achieving the bare minimal loss is frequently less important in real-world power system operation than maintaining power quality and system stability, especially when combining renewable energy sources and electric vehicle charging stations.

PSO can converge to solutions with marginally reduced power losses because of its loss-focused optimization trajectory, but it frequently overlooks secondary goals, which leads to higher THD, greater voltage imbalance, and longer computation durations. On the other hand, CLORM uses the recursive neural predictor in conjunction with the hybridized COA–LOA search approach to produce well-balanced solutions that adhere to operational restrictions while greatly enhancing computing efficiency, voltage stability, and harmonic quality. Therefore, a slight increase in power loss is a reasonable trade-off for better overall performance on all other important measures.

5.3.2. Realtime validation Even if the CLORM framework performs well in IEEE 33-bus simulations, real-world operating conditions must be validated before it can be used in practice. Because they are unable to accurately represent the changes in renewable Energy, consumer charging behavior, governmental restrictions, and socioeconomic issues that affect the adoption of EVCS, simulated environments are by their very nature limited. Collaborations with utilities and grid operators are essential to closing this gap. Pilot experiments using regional grids, like the Ontario electricity system [12], for example, may offer important empirical data on the robustness, scalability, and adaptability of CLORM. In order understand the realtime feasibility, the proposed model is tested for the 118 bus system and the hardware specification also described in table 9.

Table 9. Realtime feasibility analysis

Test Network	Power Loss (MW)	THD (%)	Voltage Imbalance (%)	Computation Time (s)	Hardware Specifications
IEEE 333-bus	206.732	0.6934	1.01	0.0728	Intel i7-12700K, 16 GB RAM, no GPU
IEEE 69-bus	214.568	0.812	1.23	0.118	Intel i7-12700K, 16 GB RAM, no GPU
IEEE 118-bus	237.943	0.934	1.36	0.192	Intel i7-12700K, 16 GB RAM, no GPU

In order to make sure that the model is not only theoretically ideal but also practically feasible and socially inclusive, such partnerships would allow stress-testing against actual load patterns, voltage deviations, and equity-oriented placement strategies. Hence, the proposed model has the sufficient tuning functions for processing in the realtime environment.

6. Conclusion

The primary aim of the research is to identify the most efficient placement of EVCS within the distribution network. The efficacy of the suggested model was assessed within a hybrid DG system created in the MATLAB environment.

The analysis employed the IEEE 33 bus system to pinpoint the ideal location for an EVCS. In this framework, recursive layers evaluate the line and load data of the bus system, with the optimal site being established through the crayfish and lotus fitness methodologies. To conclude, the efficacy of the implemented methods is assessed by validating the proposed simulation results and comparing them with other contemporary techniques based on criteria such as voltage, THD, power loss, and processing time. The CLORM demonstrates a power loss of 206.7320kW, signifying effective energy utilization. The THD measures 0.6934%, indicating a high power quality with negligible distortion. Voltage imbalance stands at 1.01%, remaining within the acceptable thresholds for grid stability. The computation time recorded is 0.072788s, highlighting the processing efficiency of the CLORM approach. Future research should optimize EVCS placement strategy with realtime data and integrate machine learning for predictive analysis and decision-making.

Appendix

Algorithm 1: CLORM

Input:

    Grid data: buses, lines, loads, renewable generation forecasts.
    EVCS candidate locations.
    System constraints: branch thermal ratings, bus voltage limits, BESS, EVCS limits.
    COA parameters:
        Population size carry_fish = 50.
        Max iterations MaxIter_carry_fish = 100.
        Step size factor $\alpha = 0.5$ (for crab foraging movement).
    LOA parameters:
        Population size lotus = 30.
        Max iterations MaxIter_lotus = 80.
        Stopping criteria: Max iterations or convergence tolerance $= 1e - 5$.

Output:

    - Optimal EVCS placement and operational schedule.
    Optimal dispatch of renewable / BESS units.

1. Initialization

    a. Generate initial population of potential EVCS locations.
        For $i = 1$ to N_{coa}:
            Randomly assign EVCS locations to candidate buses.
            Evaluate feasibility w.r.t. system constraints.
            Store as individual solution X_i.
    b. Initialize COA population with X_i.
    c. Initialize tracking of best solution: $X\_$best.

2. COA Phase (Global Foraging Search)

    For iter_coa = 1 to MaxIter_coa:
    For each individual X_i in COA population:
        - Apply crab foraging strategy (see Eqn. 3):
            Evaluate fitness $f(X\_i)$ based on objective (cost, losses, voltage deviation).
            Determine foraging direction using local gradient / random perturbation.
            Update location: $X\_i\_$new $= X\_i + \alpha^*$(direction vector).
        - Enforce feasibility: clip voltage, branch, EVCS, BESS constraints.

End For

    Update $X\_$best if any $X\_i\_$new improves fitness.
    Optional: apply diversity maintenance to avoid premature convergence.
    End For

Store COA output population (e.g. X_COA_best or top solutions) for LOA input.

3. LOA Phase (Local Exploitation / Refinement)

a. Initialize LOA population with top COA solutions.

b. For iter_loa = 1 to MaxIter_loa:

For each individual Y_i in LOA population:

Apply Lotus Optimization local movement:

i. Exploit best local solution while maintaining diversity.

ii. Update positions $Y\_i\_new = Y\_i + \beta * (X\_local\_best - Y\_i)$.

Evaluate fitness $f(Y\_i\_new)$.

End For

Update LOA global best solution Y_best.

Check convergence: if $|f(Y\_best\_new) - f(Y\_best\_old)| <$ best fitness, break.

End For

4. Hybrid Interaction

COA provides global exploration output to seed LOA.

LOA performs refined local search on COA solutions.

Optionally, can iterate COA–LOA loop for K cycles for better hybridization.

5. Stopping Criteria

If MaxIter_COA and MaxIter_LOA reached, or convergence tolerance achieved.

6. Return

X_optimal = Y_best (optimal EVCS locations).

Corresponding dispatch and charging schedule for EVCS, renewable units, and BESS.

REFERENCES

1. Y. Levingstan, and K.S. Saji, "A novel two-stage game theory-based data-driven coordination control for efficient power allocation and EV charging management," Electrical Engineering, 2024. https://doi.org/10.1007/s00202-024-02809-7

2. S. Aggarwal, and A.K. Singh, "Assessing performance of EV Charging Station with siting of DERs and FACTS devices under Deregulated Environment," Electrical Engineering, vol. 105, pp. 4119–4137, 2023. https://doi.org/10.1007/s00202-023-01928-x

3. B. Gunapriya, B.S. Kumar, B. Rajalakshmi, and A. Amarendra, "Performance enhancement of EV charging stations and distribution system: a GJO–APCNN technique," Electrical Engineering, vol. 107, pp. 883–897, 2025. https://doi.org/10.1007/s00202-024-02531-4

4. J. Axsen, and J. Pickrell-Barr, "What drives fleets? Organizations' perceived barriers and motivators for alternative-fuel vehicles", Transportation Research Part D: Transport and Environment, vol. 132, pp. 104220, 2024. https://doi.org/10.1016/j.trd.2024.104220

5. M. Kumar, and S. Sharma, "Renewable Energy and Sustainable Transportation," Role of Science and Technology for Sustainable Future: Volume 1: Sustainable Development: A Primary Goal, Singapore: Springer Nature Singapore, 2024, pp. 375-414. https://doi.org/10.1007/978-981-97-0710-2_22

6. P. Barman, and L. Dutta, "Charging infrastructure planning for transportation electrification in India: A review," Renewable and Sustainable Energy Reviews, vol. 192, pp. 114265, 2024. https://doi.org/10.1016/j.rser.2023.114265

7. A.R. Singh, P. Vishnuram, S. Alagarsamy, M. Bajaj, V. Blazek, I. Damaj, R.S. Rathore, F.N. Al-Wesabi, and K.M. Othman, "Electric vehicle charging technologies, infrastructure expansion, grid integration strategies, and their role in promoting sustainable e-mobility," Alexandria Engineering Journal, vol. 105, pp. 300-330, 2024. https://doi.org/10.1016/j.aej.2024.06.093

8. K.H. Mhana, and H.A. Awad, "An ideal location selection of electric vehicle charging stations: Employment of integrated analytical hierarchy process with geographical information system," Sustainable Cities and Society, vol. 107, pp. 105456, 2024. https://doi.org/10.1016/j.scs.2024.105456

9. A. Habbal, and M.F. Alrifaie, "A User-Preference-Based Charging Station Recommendation for Electric Vehicles," IEEE Transactions on Intelligent Transportation Systems, vol. 25, no. 9, pp. 11617-11634, 2024. DOI: 10.1109/TITS.2024.3379469

10. N. Aljohani and A. Bhattacharya, "Planning of fast charging infrastructure for electric vehicles in a distribution system and prediction of dynamic price," arXiv preprint arXiv:2301.06807, 2023.

11. J. Liang, Z. Dong, and Y. Li, "Particle swarm optimization based on data driven for EV charging station siting," Energy, vol. 310, 2024.

12. W. Liu, J. Li, and T. Ma, "Data-driven optimization of EV charging station placement using causal discovery," arXiv preprint arXiv:2503.17055, Mar. 2025.

13. A. T. Santos et al., "Smart allocation and sizing of fast charging stations: a metaheuristic solution," Philosophical Magazine, vol. 104, no. 24, pp. 3875–3895, 2024.

14. R. K. Jaiswal, S. Rajasekar, and P. Prakash, "Artificial intelligence-based optimal EVCS integration with stochastically sized and distributed PVs in an RDNS segmented in zones," Journal of Electrical Systems and Information Technology, vol. 10, no. 1, pp. 1–12, Dec. 2023.

15. T. Aljohani, and A. Almutairi, "Modeling time-varying wide-scale distributed denial of service attacks on electric vehicle charging Stations," Ain Shams Engineering Journal, vol. 15, no. 7, pp. 102860, 2024. https://doi.org/10.1016/j.asej.2024.102860

16. S.S.A. Salam, V. Raj, M.I. Petra, A.K. Azad, S. Mathew, and S.M. Sulthan, "Charge Scheduling Optimization of Electric Vehicles: A Comprehensive Review of Essentiality, Perspectives, Techniques and Security," IEEE Access, vol. 12, pp. 121010-121034, 2024. DOI: 10.1109/ACCESS.2024.3433031

17. F. Ahmad, and M. Bilal, "Allocation of plug-in electric vehicle charging station with integrated solar powered distributed generation using an adaptive particle swarm optimization," Electrical Engineering, vol. 106, no. 3, pp. 2595-2608, 2024. https://doi.org/10.1007/s00202-023-02087-9

18. R. Sepehrzad, A. Khodadadi, S. Adinehpour, and M. Karimi, "A Multi-Agent Deep Reinforcement Learning Paradigm to Improve the Robustness and Resilience of Grid Connected Electric Vehicle Charging Stations against the Destructive Effects of Cyber-attacks," Energy, vol. 307, pp. 132669, 2024. https://doi.org/10.1016/j.energy.2024.132669

19. M. Khalid, J. Thakur, S.M. Bhagavathy, and M. Topel, "Impact of public and residential smart EV charging on distribution power grid equipped with storage," Sustainable Cities and Society, vol. 104, pp. 105272, 2024. https://doi.org/10.1016/j.scs.2024.105272

20. K. Balu, and V. Mukherjee, "Optimal deployment of electric vehicle charging stations, renewable distributed generation with battery energy storage and distribution static compensator in radial distribution network considering uncertainties of load and generation," Applied Energy, vol. 359, pp. 122707, 2024. https://doi.org/10.1016/j.apenergy.2024.122707

21. R. Ildarabadi, H. Lotfi, M.E. Hajiabadi, and M.H. Nikkhah, "Presenting a new mathematical modeling for distribution network resilience based on the optimal construction of tie-lines considering importance of critical electrical loads," Electrical Engineering, vol. 106, no. 3, pp. 2503-2524, 2024. https://doi.org/10.1007/s00202-023-02077-x

22. M.N. Babu, and P.K. Dhal, "Impact of load flow and network reconfiguration for unbalanced distribution systems," Measurement: Sensors, vol. 32, pp. 101078, 2024. https://doi.org/10.1016/j.measen.2024.101078

23. S. Maji, and P. Kayal, "A simplified multi-objective planning approach for allocation of distributed PV generators in unbalanced power distribution systems," Renewable Energy Focus, vol. 48, pp. 100541, 2024. https://doi.org/10.1016/j.ref.2024.100541

24. E.A. Rene, and W.S.T. Fokui, "Artificial intelligence-based optimal EVCS integration with stochastically sized and distributed PVs in an RDNS segmented in zones," Journal of Electrical Systems and Information Technology, vol. 11, no. 1, pp. 1, 2024. https://doi.org/10.1186/s43067-023-00126-w

25. J. Wang, Q. Guo, and H. Sun, "Planning approach for integrating charging stations and renewable energy sources in low-carbon logistics delivery," Applied Energy, vol. 372, pp. 123792, 2024. https://doi.org/10.1016/j.apenergy.2024.123792

26. S. Ray, K. Kasturi, S. Patnaik, and M.R. Nayak, "Review of electric vehicles integration impacts in distribution networks: Placement, charging/discharging strategies, objectives and optimization models," Journal of Energy Storage, vol. 72, pp. 108672, 2023. https://doi.org/10.1016/j.est.2023.108672

27. M.M. Hamed, D.M. Kabtawi, A. Al-Assaf, O. Albatayneh, and E.S. Gharaibeh, "Random parameters modeling of charging-power demand for the optimal location of electric vehicle charge facilities," Journal of Cleaner Production, vol. 388, pp. 136022, 2023. https://doi.org/10.1016/j.jclepro.2023.136022

28. Z. Yang, F. Yang, H. Min, H. Tian, W. Hu, J. Liu, and N. Eghbalian, "Energy management programming to reduce distribution network operating costs in the presence of electric vehicles and renewable energy sources," Energy, vol. 263, pp. 125695, 2023. https://doi.org/10.1016/j.energy.2022.125695

29. M. Abdel-Basset, A. Gamal, I.M. Hezam, and K.M. Sallam, "Sustainability assessment of optimal location of electric vehicle charge stations: a conceptual framework for green energy into smart cities," Environment, Development and Sustainability, vol. 26, no. 5, pp. 11475-11513, 2024. https://doi.org/10.1007/s10668-023-03373-z

30. A. Charly, N.J. Thomas, A. Foley, and B. Caulfield, "Identifying optimal locations for community electric vehicle charging," Sustainable Cities and Society, vol. 94, pp. 104573, 2023. https://doi.org/10.1016/j.scs.2023.104573

31. M.M. Hasan, M.A. Yousuf, and M.R. Islam, "Management of EVs for Mitigating Unbalance in a LV Distribution Grid," 2024 6th International Conference on Electrical Engineering and Information & Communication Technology (ICEEICT), IEEE, 2024. DOI: 10.1109/ICEEICT62016.2024.10534474

32. W. Alabri, and D. Jayaweera, "Optimal coordination of unbalanced power distribution systems with integrated photovoltaic systems and semi-fast electric vehicles charging stations," IET Generation, Transmission & Distribution, vol. 16, no. 12, pp. 2399-2415, 2022. https://doi.org/10.1049/gtd2.12458

33. J.B. Bernal-Vargas, J.C. Castro-Galeano, E.E. Tibaduiza-Rincón, J.M. López-Lezama, and N. Muñoz-Galeano, "Prospective analysis of massive integration of electric vehicle chargers and their impact on power quality in distribution networks," World Electric Vehicle Journal, vol. 14, no. 12, pp. 324, 2024. https://doi.org/10.3390/wevj14120324

34. M.S. Arjun, N. Mohan, K.R. Sathish, A. Patil, and G. Thanmayi, "Impact of electric vehicle charging station on power quality," International Journal of Applied Power Engineering, vol. 13, no. 1, pp. 186-193, 2024. DOI: 10.11591/ijape.v13.i1.pp186-193

35. E.A. Rene, W.S.T. Fokui, and P.K.N. Kouonchie, "Optimal allocation of plug-in electric vehicle charging stations in the distribution network with distributed generation," Green Energy and Intelligent Transportation, vol. 2, no. 3, pp. 100094, 2023. https://doi.org/10.1016/j.geits.2023.100094

36. M. Altaf, M. Yousif, H. Ijaz, M. Rashid, N. Abbas, M.A. Khan, M. Waseem, and A.M. Saleh, "PSO-based optimal placement of electric vehicle charging stations in a distribution network in smart grid environment incorporating backward forward sweep method," IET Renewable Power Generation, vol. 18, no. 15, pp. 3173-3187, 2024. https://doi.org/10.1049/rpg2.12916

37. K. Kathiravan, and P.N. Rajnarayanan, "Application of AOA algorithm for optimal placement of electric vehicle charging station to minimize line losses," Electric Power Systems Research, vol. 214, pp. 108868, 2023. https://doi.org/10.1016/j.epsr.2022.108868

38. H. Jia, X. Zhou, J. Zhang, L. Abualigah, A.R. Yildiz, and A.G. Hussien, "Modified crayfish optimization algorithm for solving multiple engineering application problems," Artificial Intelligence Review, vol. 57, no. 5, pp. 127, 2024. https://doi.org/10.1007/s10462-024-10738-x

39. E. Dalirinia, M. Jalali, M. Yaghoobi, and H. Tabatabaee, "Lotus effect optimization algorithm (LEA): a lotus nature-inspired algorithm for engineering design optimization," The Journal of Supercomputing, vol. 80, no. 1, pp. 761-799, 2024. https://doi.org/10.1007/s11227-023-05513-8